

## Plasma wall interaction during ELMs in JET

E. Gauthier <sup>a,\*</sup>, P. Andrew <sup>b</sup>, G. Arnoux <sup>a</sup>, Y. Corre <sup>a</sup>,  
H. Roche <sup>a</sup>, JET-EFDA Contributors

<sup>a</sup> Association EURATOM-CEA, CEA/DSM/DRFC, CEA Cadarache, 13108 Saint Paul Lez Durance, France

<sup>b</sup> Euratom/UKAEA Fusion Association, Culham Science Centre, Abingdon OX14 3DB, UK

---

### Abstract

Particle and energy fluxes during transient events such as ELMs (edge localized modes) and disruptions need to be controlled to prevent damage to the Plasma Facing Components. A new wide angle infrared and visible diagnostic has been installed on JET which permits the observation of the plasma wall interaction in the main chamber. First observations of the interaction of ELMs with the main chamber are presented. Areas of interaction vary with the magnetic configuration and also within a single shot. A part of the ELM energy is deposited outside the divertor, mainly on the inner baffle, the outer limiter and the upper limiters.

© 2007 Published by Elsevier B.V.

*PACS:* 52.40.Hf; 52.55.Fa; 52.55.Rk; 52.70.–m

*Keywords:* ITER; JET; ELMs; IR-thermography; Heat load

---

### 1. Introduction

Heat load deposition on Plasma Facing Components (PFC) is one of the main issues for ITER. Today, due to its good thermal–physical properties, carbon is proposed for the main plasma interaction area in the divertor. Tungsten, in order to minimize tritium retention in the codeposited layers, is proposed for the other parts of the divertor, where particles and power flux are expected to be lower, while beryllium is used on the first wall. This complex configuration is based on a plasma scenario where heat

load deposition is well defined and controlled. If the heat load on PFC is well known during the steady phases of the plasma, this is not the case during the transient events such as ELMs and disruption. Depending of the localisation and the intensity of the energy deposited during ELMs, the choice of the materials may have to be reconsidered in ITER.

In the frame of the JET-EP (enhanced programme), a new infrared thermography diagnostic has been designed [1] and installed on JET during the 2004–2005 shutdown. This system is a unique diagnostic; able to provide a wide angle view in the visible and in the infrared, for thermography of the main chamber and divertor and for analysis of the power and energy fluxes deposition during steady phases and transient events.

---

\* Corresponding author. Tel.: +33 4 42 25 42 04; fax: +33 4 42 25 49 90.

E-mail address: [eric.gauthier@cea.fr](mailto:eric.gauthier@cea.fr) (E. Gauthier).

## 2. The wide angle infrared and visible diagnostic

In order to image a large section of the tokamak both in poloidal and toroidal directions, the optical system has been designed with a field of view of  $70^\circ$ , allowing the observation of the divertor, the inner wall, the ICRF antennae and the upper limiter. A very important aim of the diagnostic is to be ITER relevant. To this end, the optical components are mainly reflective, metallic aspheric mirrors; being the only kind which can sustain high neutron irradiation. The diagnostic is composed of an endoscope,

equipped with the front mirrors at one end (both mirrors are made of stainless steel coated with gold), a Cassegrain telescope (made of aluminium mirrors coated with gold) at the other end and an infrared camera (see Fig. 1). A part of the photon flux is extracted from the Cassegrain telescope and is transmitted via a 200 mm lens to a CCD camera, providing the same field of view in the visible and in the infrared range, seen in Fig. 2, which shows the internal components of the JET vessel. The IR diagnostic is able to measure a large dynamic range; from room temperature up to a maximum of

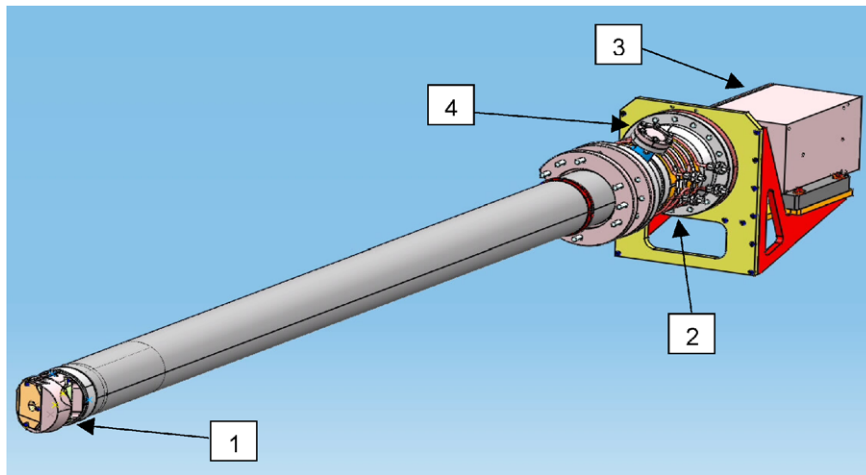


Fig. 1. Opto-mechanical design of the wide angle infrared and visible diagnostic: (1) Front mirrors; (2) Cassegrain telescope; (3) IR camera; (4) Visible port.

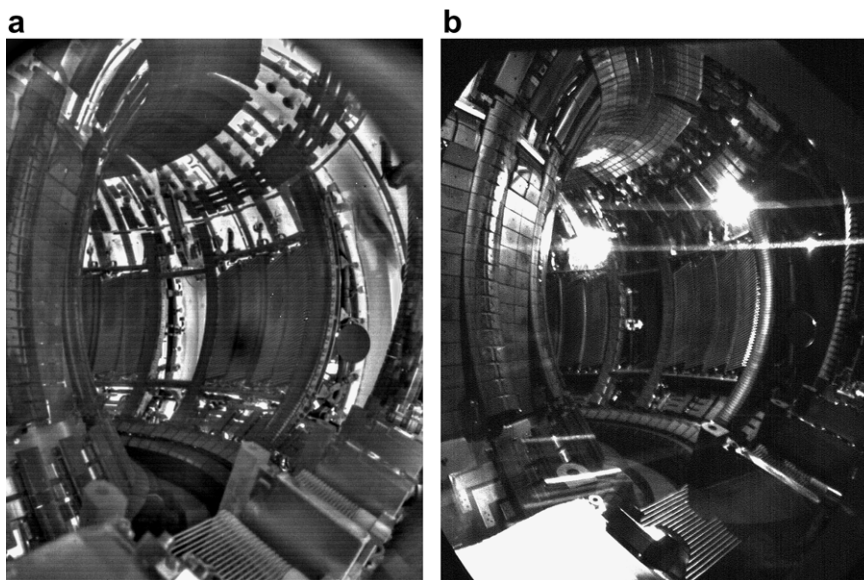


Fig. 2. Internal view of the JET vessel in the (a) infrared and (b) the visible range.

2000 °C, within a single shot, by using several exposure times and two different filters (wide: 4.2–4.4  $\mu\text{m}$  and narrow: 3.97–4.01  $\mu\text{m}$ ). The infrared camera is equipped with a MCT (mercury–cadmium–tellurium) detector working in the 3.6–5.1  $\mu\text{m}$  range and cooled at 80 K by means of a stirling cooler. The focal plane array comprises  $640 \times 512$  pixels. All pixels are exposed at the same time (snapshot mode) with an exposure time variable between 20  $\mu\text{s}$  and 10 ms. The minimum exposure time of 20  $\mu\text{s}$  allows the ‘freezing’ of fast events such as ELMs and disruptions within a single frame. The maximum frame rate is 100 Hz for a full size image, which can be increased to 10 kHz by reducing the number of pixels. This provides a time resolution of 100  $\mu\text{s}$  and allows the accurate measurements of the energy deposited during ELMs. The spatial resolution of the optics and the camera is 6 mm at a distance of 3 m (distance to the inner wall and to the outer limiter).

### 3. Results

The first results on the plasma wall interaction during ELMs have been recently obtained during the restart operations, prior to the JET experimental campaign. The Fig. 3 shows an infrared image of the JET vessel during an ELMy discharge, where several areas have been selected on the inner wall, the inner divertor, the outer divertor, the upper limiter, the outer limiter and the ICRF antenna. The average temperatures within these areas are plotted as function of time. The spikes on temperatures,

observed mainly on the inner and outer divertor, are correlated with the  $\text{H}\alpha$  signal and are due to the ELMs. Some interaction occurs also on the ICRF antenna but no effect is visible on the inner wall neither on the upper limiter. The temperature increase is more pronounced on the inner wall due to the combined effect of the ELM energy deposited and the codeposited layer, which is mainly located on the inner divertor in JET (in normal magnetic field configuration) [2]. These codeposited layers, with low thermal conductivity induce an offset in temperature during exposure to high heat flux [3]. The location of the ELM interaction with the main chamber may vary from a shot to another one, in particular with the magnetic configuration. Fig. 4 shows the increase of the temperature during to a single ELM for two different configurations. These images are obtained from the difference of two consecutive frames: one before the ELM, one after the ELM. The time resolution being not sufficient to resolve ELMs, the real increase in temperature is higher than the measured value depending of the delay between the ELM event and the exposure of the camera. For the shot 66030, with both strike points on the horizontal target, the ELM interaction is located mainly on the inner divertor (temperature on outer divertor not measured) and on the outer limiter with an increase of the temperature of 700 °C and 300 °C, respectively. During the shot 66224, with high triangularity, low X-point (HDLX) configuration, the ELM interaction is mainly located on the inner divertor and on the upper limiter with an increase of the temperature

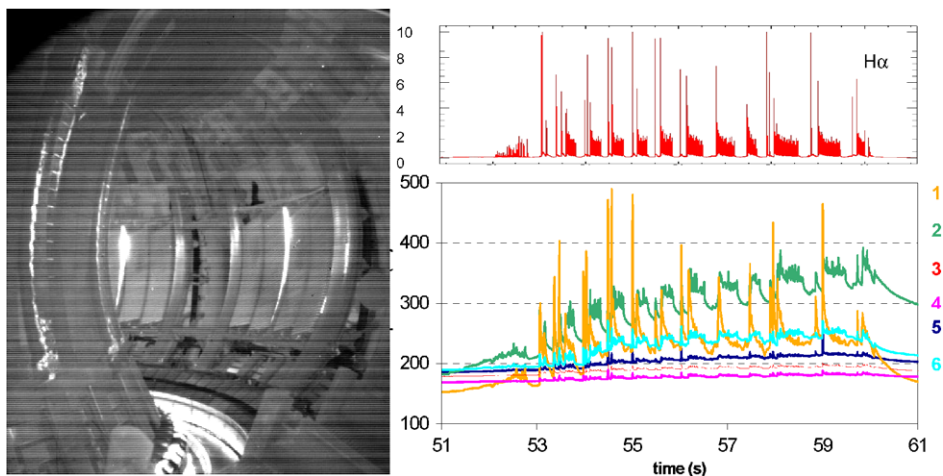


Fig. 3. IR image during an ELMy discharge,  $\text{H}\alpha$  signal and average temperature evolution on the (1) inner divertor, (2) outer divertor, (3) inner wall, (4) upper limiter, (5) outer limiter and (6) ICRF antenna.

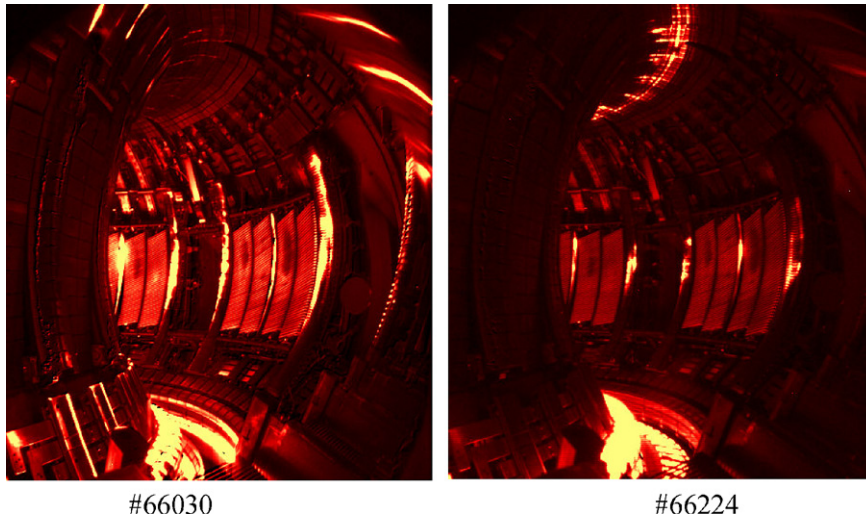


Fig. 4. IR views of an ELM during a discharge with standard magnetic configuration (#66030) and with high triangularity, lower X-point configuration (#66224).

of 1100 °C and 500 °C, respectively. These temperature increases have been measured on several shots (see Table 1) with a plasma stored energy of about 6 MJ and with an average ELM energy of about 0.2 MJ. At present, the modeling of the main chamber tiles is in progress, the calculation of the energy deposited outside the divertor is not available, and so the fraction of the ELM energy deposited on the different PFC cannot yet be quantified.

Independent of the influence of the magnetic configuration, ELM interaction with the main chamber may vary during a single shot. Fig. 5 shows the time evolution of the temperature on the inner divertor, outer divertor, outer limiter and upper limiter. It can be seen that in most of the case the maximum

temperature increase due to the ELMs is located on the inner divertor, some ELMs have a different behaviour, inducing a large increase in temperature on the outer limiter in standard configuration and on the upper limiter in the HDLX configuration. This non uniformity in the ELMs interaction with the main chamber is not correlated, at present, with any other signal and no explanation has yet been proposed for these variations in the interaction area.

Even though the frame rate used during these experiments (maximum 1 kHz) is too low to provide time resolution during an ELM, the short exposure time, combined with a statistical analysis on hundreds of ELMs from the list in Table 1, allows information to be provided on the short time scale of an

Table 1

Main parameter of the analysed discharges: toroidal field ( $B_t$ ), plasma current ( $I_p$ ), injected neutral beam power (NBI), injected RF power (ICRH), plasma stored energy ( $W_{\text{dia}}$ ), magnetic configuration (config) where HDLX means high triangularity, low X-point, vertical means strike points on vertical targets, horizontal means strike points on horizontal targets, vert/hor means inner strike point on vertical target and outer strike point on horizontal target, IR camera time resolution ( $\tau_{\text{IR}}$ ), IR camera exposure time ( $\tau_{\text{acqui}}$ ) and variation of surface temperature during ELM on inner and outer divertor, outer and upper limiters

Shot	$B_t$ (T)	$I_p$ (MA)	NBI (MW)	ICRH (MW)	$W_{\text{dia}}$ (MJ)	Config	$\tau_{\text{IR}}$ (ms)	$\tau_{\text{acqui}}$ ( $\mu$ s)	$\Delta T$ ELMs (max)			
									Inner div.	Outer div.	Outer lim.	Upper lim.
66265	2.7	2.5	17.7	3.6	6.2	HDLX	20	300	800	300	100	650
66232	2.8	2.6	12.9	2/3.6	5	Vertical	6	60	350	400	700	
66224	2.7	2.5	14.8	2.7		HDLX	8	60	1100	500		600
66030	3	1.5	15		3	Vertical	10	600	700	Sat	300	
66013	3	2.5	14	6	6	Horizontal	20	300	450	700	250	
65929	2.55	2	12	1	6	Vert/hor	1	300	600	250		
65740	2.6	2	9.7	3.4		Vert/hor	3	300	300	800	40	170

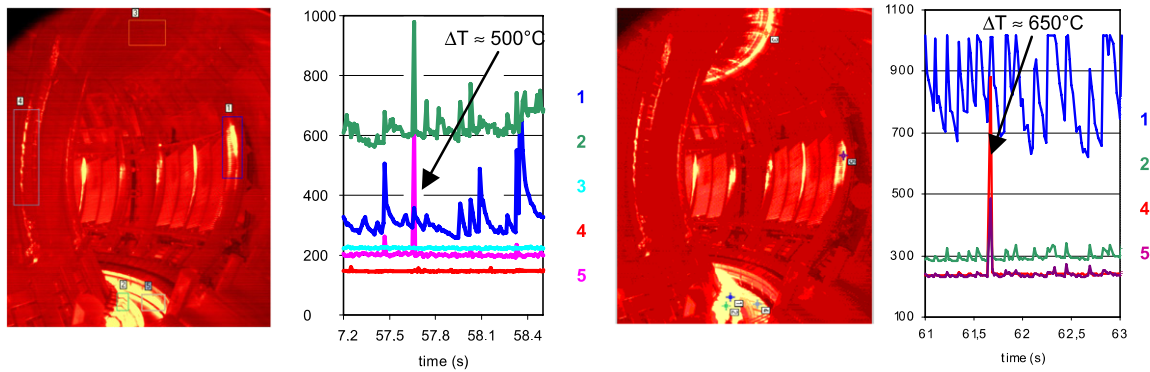


Fig. 5. IR views and PFC temperature evolution on the (1) inner divertor, (2) outer divertor, (3) inner wall, (4) upper limiter, (5) outer limiter during discharges with two different magnetic configurations.

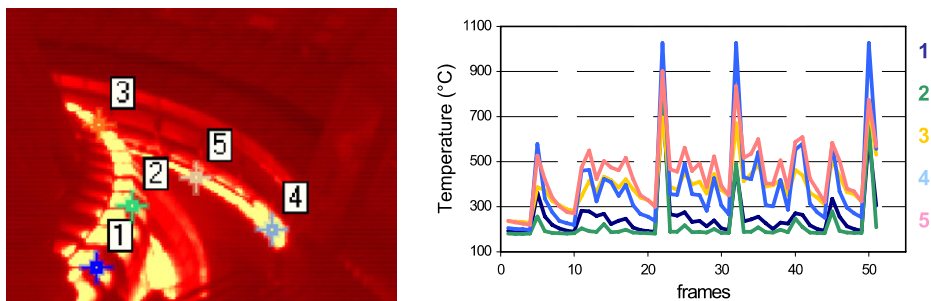


Fig. 6. Divertor IR view and temperature evolution at several locations on inner and outer divertor.

individual ELM. Fig. 6 shows the temperature evolution of several point distributed on toroidal direction on inner and outer divertor. All points exhibit an increase in temperature in the same frame, not only for these ELMs but for all ELMs observed. Thanks to the exposure of all pixels at the same time, it can be concluded that all points are exposed to the ELM energy at the same time, within  $60 \mu\text{s}$  (the minimum exposure time used so far). This result would indicate that the heat deposition during an ELM is faster than the sound speed and therefore must be driven by fast electrons. This result is in agreement with previous observations by Chan-kin on JT-60U [4], where no delay or a delay smaller than  $50 \mu\text{s}$  were observed on  $\text{H}\alpha$  signals on inner and outer divertor. This preliminary result should be confirmed by further measurement performed with a shorter exposure time ( $20 \mu\text{s}$ ).

#### 4. Conclusions

An ITER-like infrared thermography and visible viewing diagnostic has been installed on JET. The wide angle view allows the observation of the inner

wall, the divertor, the outer and upper limiter and the ICRF antennae. First IR images obtained during ELMy discharges showed that the plasma wall interactions are not only localized in the divertor, during ELMs, but a part of the ELMs energy is also deposited on the upper and outer limiters. No interaction is observed on the inner wall during ELMs, in contrast to the disruptions, where most of the energy is deposited on the inner wall [5]. The areas of the ELM interaction vary with the magnetic configuration and the intensity of the ELMS interaction with the main chamber varies also within a single shot. The increase in temperature occurs simultaneously on the inner and outer divertor and in toroidal direction, within a time scale of  $60 \mu\text{s}$ , which would indicate that the heat load during the ELMs is driven by fast electrons.

#### Acknowledgement

This work has been performed under the European Fusion Development Agreement in the frame of the Contract EFDA04-1180.

## References

- [1] E. Gauthier et al., in: Proc. of 32nd EPS Conf. on Plasma Phys., Tarragona 2005, ECA, vol. 29C, 2005.
- [2] P. Andrew et al., *J. Nucl. Mater.* 313–316 (2003) 135.
- [3] E. Gauthier et al., *J. Nucl. Mater.* 337–339 (2005) 960.
- [4] A. Chankin et al., *Nucl. Fusion* 42 (1992) 733.
- [5] P. Andrew et al., *J. Nucl. Mater.*, these Proceedings, doi:10.1016/j.jnucmat.2007.01.285.